

Two-Photon Spectroscopy of a Series of Platinum Acetylides: Conformation-Induced Ground-State Symmetry Breaking

Thomas M. Cooper,^{*,†} Joy E. Haley,[†] Douglas M. Krein,[‡] Aaron R. Burke,[‡] Jonathan E. Slagle,[§] Aleksandr Mikhailov,^{||} and Aleksander Rebane^{*,||,⊥}

[†]Materials and Manufacturing Directorate, Air Force Research Laboratory, Wright-Patterson Air Force Base, Dayton, Ohio 45433, United States

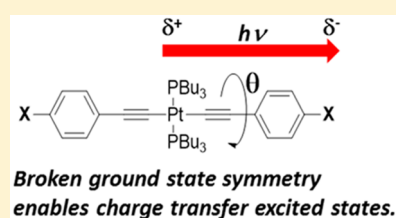
[‡]General Dynamics Information Technology, Dayton, Ohio 45431, United States

[§]Slagle Photonics, Dayton, Ohio 45433, United States

^{||}Physics Department, Montana State University, Bozeman, Montana 59717, United States

[⊥]National Institute of Chemical Physics and Biophysics, Tallinn 12618, Estonia

ABSTRACT: With the goal of elucidating electronic and conformational effects on structure–spectroscopic property relationships in platinum acetylides, we synthesized a series of nominally centrosymmetric chromophores $trans\text{-Pt}(\text{PBu}_3)_2(\text{C}\equiv\text{C-Phenyl-X})_2$, where X = diphenylamino (DPA), NH_2 , OCH_3 , $t\text{-Bu}$, CH_3 , H, F, benzothiazole (BTH), CF_3 , CN, and NO_2 . We collected one- and two-photon absorption spectra and also performed density functional theory (DFT) and time-dependent (TD) DFT calculations on the ground- and excited-state properties of these compounds. The DFT calculations revealed facile rotation between the two ligands, suggesting that the compounds exhibit nonplanar ground-state conformations in solution. TDDFT calculation of the S_1 state energy and transition dipole moment for a nonplanar conformation gave good agreement with experiment. Two-photon absorption spectra obtained from these compounds allowed estimation of the change of permanent electric dipole moment upon vertical excitation from ground state to S_1 state. The values are small $\Delta\mu < 1.0$ D for neutral substituents such as CH_3 , H, and F but increase sharply to $\Delta\mu \approx 11$ D for electron-accepting NO_2 . When in a nonplanar conformation, the corresponding calculated $\Delta\mu$ values showed good agreement with the experimental data indicating that the two-photon spectra result from nonplanar ground-state conformations. Previously studied related chromophores having extended conjugation (Rebane, A.; Drobizhev, M.; Makarov, N. S.; Wicks, G.; Wnuk, P.; Stepanenko, Y.; Haley, J. E.; Krein, D. M.; Fore, J. L.; Burke, A. R.; Slagle, J. E.; McLean, D. G.; Cooper, T. M. *J. Phys. Chem. A* **2014**, *118*, 3749–3759) show similar dependence of $\Delta\mu$ on the substituents, which allows us to conclude that the excited-state properties of these floppy chromophores are a function of the electronic properties of the substituents, ligand size, and nonplanar molecular conformation.



INTRODUCTION

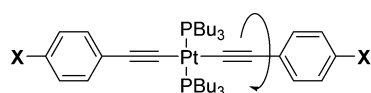
Platinum acetylides are known to exhibit exceptional photophysical properties, which has stimulated continuing structure–property investigations.^{1–9} Over the last two decades, there have been research published on excited-state phenomena including ground- and excited-state absorption, phosphorescence, intersystem crossing, triplet-state absorption, two-photon absorption (2PA),^{10–13} three-photon absorption,¹⁴ formation of excimers,¹⁵ and two-beam coupling.¹⁶ We recently reported on the synthesis and photophysical characterization of a series of platinum(II) *trans*-bis(tributylphosphine)-bis(4-((9,9-diethyl-7-ethynyl-9H-fluoren-2-yl)ethynyl)-X) complexes, $\text{Pt}(\text{FL-R-X})_2$, where FL-R-X stands for the ligand containing an end group X with a range of electron-donating and electron-accepting characteristics.^{17–19} We found their ground- and excited-state behavior to be a strong function of conformation as well as electronic effects. In particular, we observed that even if the molecular structure is nominally close to centrosymmetric, the presence of potent electron-accepting end groups such as benzothiazole (BTH), CN, and NO_2 imposes a

behavior resembling that of strongly dipolar chromophores. While lowering of symmetry in molecular excited states is a rather common phenomenon, evidence supporting spontaneous symmetry-breaking in the ground state remains relatively scarce.²⁰ To understand how the conformation, ligand length, and electronic effects influence the spectroscopic behavior of platinum acetylides, we synthesized a parallel series of $trans\text{-Pt}(\text{PBu}_3)_2(\text{C}\equiv\text{C-Phenyl-X})_2$ having the molecular formula shown in Scheme 1. In comparison to $\text{Pt}(\text{FL-R-X})_2$ series, current $\text{Pt}(\text{R-X})_2$ structures possess a compact (and presumably less complex) conjugation framework. This attribute was designed to provide a more clear indication of the symmetry-breaking effect and its underlying causes. We collected ground-state absorption as well as 2PA spectra, where the latter provided insight about molecular symmetry via alternative parity selection rule. We also performed density

Received: May 17, 2017

Revised: June 22, 2017

Published: June 26, 2017

Scheme 1. Molecular Formula of Platinum Acetylide Pt-(R-X)₂ Series^a

X = NH₂, OCH₃, DPA, *t*-Bu, CH₃, H, F, BTH, CF₃, CN, NO₂

^aDPA = diphenyl amino, BTH = benzothiazole. The angle θ is the angle between the two phenyl ring planes. The compounds are identified by the names of the end caps (X).

functional theory (DFT) and time-dependent (TD) DFT calculations on the ground- and excited-state properties of Pt-(R-X)₂ including identification of possible conformations. On the basis of good quantitative correspondence between calculations and experimental findings, we conclude that the spectroscopic behavior of platinum acetylides is a function of electronic effects from the substituent and conformational effects due to free rotation about the C≡C bond, and these compounds exhibit nonplanar conformation in solution.

EXPERIMENTAL SECTION

Compound **H** and all the other compounds were synthesized according to published methods.¹

NH₂: *trans*-Bis(tributylphosphine)-bis(4-amino-phenylethynyl)platinum ¹H NMR (300 MHz, CDCl₃) δ 8.12(d, *J* = 9.0 Hz, 4H), 7.40(d, *J* = 9.0 Hz, 4H), 2.13(m, 12H), 1.62(m, 12H), 1.48(m, *J* = 7.2 Hz, 12H), 0.95(t, *J* = 7.2 Hz, 18H); ¹³C NMR (75 MHz, CDCl₃) δ 143.99, 132.03, 119.77, 115.09, 108.78, 104.36("false t", *J* = 14.5 Hz), 26.62, 24.69(t, *J* = 7.1 Hz), 24.35(t, *J* = 17.1 Hz), 14.12; ³¹P NMR (121 MHz, CDCl₃) δ 3.84 (*J*_{Pt-P} = 2375 Hz); IR (KBr) ν 2107.9 cm⁻¹ Pt-C≡C; electron impact mass spectrometry (EIMS) calcd. [M+]⁺831.43; found [M+]⁺831.43; Anal. Calcd for C₄₀H₆₆N₂P₂Pt: C, 57.74%; H, 8.00%; N, 3.37%. Found: C, 57.94%; H, 7.78%; N, 3.46%.

OCH₃: *trans*-Bis(tributylphosphine)-bis(4-methoxy-phenylethynyl)platinum ¹H NMR (300 MHz, CDCl₃) δ 7.23(d, *J* = 8.7 Hz, 4H), 6.79(d, *J* = 8.7 Hz, 4H), 3.81(s, 6H), 2.19(m, 12H), 1.64(m, 12H), 1.49(m, *J* = 7.2 Hz, 12H), 0.95(t, *J* = 7.2 Hz, 18H); ¹³C NMR (75 MHz, CDCl₃) δ 157.34, 132.09, 122.05, 113.71, 108.30, 105.62 ("false t", *J* = 14.6 Hz), 55.47, 26.62, 24.68 (t, *J* = 6.6 Hz), 24.14 (t, *J* = 17.1 Hz), 14.09; ³¹P NMR (121 MHz, CDCl₃) δ 4.00 (*J*_{Pt-P} = 2370 Hz); IR (KBr) ν 2106.0 cm⁻¹ Pt-C≡C; EIMS calcd. [M+]⁺862.01; found [M+]⁺862; Anal. Calcd for C₄₂H₆₈O₂P₂Pt: C, 58.52%; H, 7.95%; O, 3.71%. Found: C, 57.79%; H, 7.8%; O, 3.98%.

DPA: *trans*-Bis(tributylphosphine)-bis(4-*N,N*-diphenyl-phenylethynyl)platinum ¹H NMR (300 MHz, CDCl₃) δ 7.25(m, 10H), 7.14(m, 10H), 7.00(m, 8H), 2.2(m, 12H), 1.66(m, 12H), 1.50(m, *J* = 7.2 Hz, 12H), 0.97(t, *J* = 7.2 Hz, 18H); ¹³C NMR (75 MHz, CDCl₃) δ 148.10, 144.94, 131.91, 129.39, 124.32, 124.20, 124.03, 122.67, 108.78, 107.63("false t", *J* = 14.6 Hz), 26.64, 24.72(t, *J* = 6.6 Hz), 24.14(t, *J* = 17.1 Hz), 14.14; ³¹P NMR (121 MHz, CDCl₃) δ 3.94 (*J*_{Pt-P} = 2365 Hz); IR (KBr) ν 2098.0 cm⁻¹ Pt-C≡C; EIMS calcd. [M+]⁺1136.37; found [M+]⁺1136; Anal. Calcd for C₆₄H₈₂N₂P₂Pt: C, 67.64%; H, 7.27%; N, 2.47%. Found: C, 67.64%; H, 7.35%; N, 2.33%.

***t*-Bu**: *trans*-Bis(tributylphosphine)-bis(4-*t*-butyl-phenylethynyl)platinum ¹H NMR (300 MHz, CDCl₃) δ 7.26(s, 8H), 2.18(m, 12H), 1.65(m, 12H), 1.60(m, *J* = 7.2 Hz, 12H),

1.34(s, 9H), 0.98(t, *J* = 7.2 Hz, 18H); ¹³C NMR (75 MHz, CDCl₃) δ -147.82, 130.68, 126.56, 125.02, 108.80, 107.17("false t", *J* = 14.6 Hz), 34.72, 31.58, 26.65, 24.70(t, *J* = 6.6 Hz), 24.09(t, *J* = 17.1 Hz), 14.15; ³¹P NMR (121 MHz, CDCl₃) δ 4.11 (*J*_{Pt-P} = 2369 Hz); IR (KBr) ν 2101.7 cm⁻¹ Pt-C≡C; EIMS calcd. [M+]⁺914.17; found [M+]⁺914; Anal. Calcd for C₄₈H₈₀P₂Pt: C, 63.06%. Found: C, 63.1%.

CH₃: *trans*-Bis(tributylphosphine)-bis(4-methyl-phenylethynyl)platinum ¹H NMR (300 MHz, CDCl₃) δ 7.22(d, *J* = 7.8 Hz, 4H), 7.05(d, *J* = 7.8 Hz, 4H), 2.34(s, 6H), 2.18(m, 12H), 1.66(m, 12H), 1.50(m, *J* = 7.2 Hz, 12H), 0.97(t, *J* = 7.2 Hz, 18H); ¹³C NMR (75 MHz, CDCl₃) δ 134.60, 130.90, 128.85, 126.44, 108.91, 107.00("false t", *J* = 14.5 Hz), 26.64, 24.69(t, *J* = 7.1 Hz), 24.15(t, *J* = 17.1 Hz), 21.56, 14.11; ³¹P NMR (121 MHz, CDCl₃) δ 4.11 (*J*_{Pt-P} = 2366 Hz); IR (KBr) ν 2101.0 cm⁻¹ Pt-C≡C; EIMS calcd. [M+]⁺830.01; found [M+]⁺830; Anal. Calcd for C₄₂H₆₈P₂Pt: C, 60.78%; H, 8.26%. Found: C, 60.53%; H, 7.96%.

F: *trans*-Bis(tributylphosphine)-bis(4-fluoro-phenylethynyl)platinum ¹H NMR (300 MHz, CDCl₃) δ 7.28(d, *J* = 5.7 Hz, 2H), 7.25(d, *J* = 5.7 Hz, 2H), 6.93(t, *J* = 5.7 Hz, 4H), 2.18(m, 12H), 1.66(m, 12H), 1.50(m, *J* = 7.2 Hz, 12H), 0.97(t, *J* = 7.2 Hz, 18H); ¹³C NMR (75 MHz, CDCl₃) δ 160.80(d, *J* = 244.6 Hz), 132.32(d, *J* = 7.5 Hz), 125.40(d, *J* = 3.0 Hz), 115.07(d, *J* = 21.6 Hz), 107.86, 107.35("false t", *J* = 14.7 Hz), 26.63, 24.68(t, *J* = 6.6 Hz), 24.21(t, *J* = 17.1 Hz), 14.03; ³¹P NMR (121 MHz, CDCl₃) δ 4.29 (*J*_{Pt-P} = 2357 Hz); IR (KBr) ν 2107.9 cm⁻¹ Pt-C≡C; EIMS calcd. [M+]⁺837.94; found [M+]⁺838; Anal. Calcd for C₄₀H₆₂F₂P₂Pt: C, 57.33%; H, 7.46%; F, 4.53%. Found: C, 57.2%; H, 7.35%; F, 4.29%.

BTH: *trans*-Bis(tributylphosphine)-bis(4-(2-benzo[*d*]-thiazole-phenylethynyl)platinum ¹H NMR (300 MHz, CDCl₃) δ 8.00(m, 8H), 7.50(m, 2H), 7.39(m, 6H), 2.18(m, 12H), 1.66(m, 12H), 1.50(m, *J* = 7.2 Hz, 12H), 0.98(t, *J* = 7.2 Hz, 18H); ¹³C NMR (75 MHz, CDCl₃) δ 168.47, 154.54, 135.24, 132.23, 131.46, 130.12, 127.46, 126.49, 125.16, 123.22, 121.78, 113.78("false t", *J* = 14.6 Hz), 109.82, 26.65, 24.69(t, *J* = 6.6 Hz), 24.27(t, *J* = 17.1 Hz), 14.09; ³¹P NMR (121 MHz, CDCl₃) δ 4.43 (*J*_{Pt-P} = 2338 Hz); IR (KBr) ν 2095.4 cm⁻¹ Pt-C≡C; EIMS calcd. [M+]⁺1068.3; found [M+]⁺1068; Anal. Calcd for C₅₄H₇₀N₂P₂S₂Pt: C, 60.71%; H, 6.48%; N, 2.62%; S, 6.00%. Found: C, 60.53%; H, 6.51%; N, 2.71%; S, 5.78%.

CF₃: *trans*-Bis(tributylphosphine)-bis(4-trifluoromethyl-phenylethynyl)platinum ¹H NMR (300 MHz, CDCl₃) δ 7.48(m, *J* = 8.1 Hz, 4H), 7.36(m, *J* = 8.1 Hz, 4H), 2.15(m, 12H), 1.64(m, 12H), 1.48(m, *J* = 7.5 Hz, 12H), 0.96(t, *J* = 7.5 Hz, 18H); ¹³C NMR (75 MHz, CDCl₃) δ 132.85(q, *J* = 1.1 Hz), 130.95, 126.70(q, *J* = 32.3 Hz), 125.09(q, *J* = 3.5 Hz), 124.80(q, *J* = 271.4 Hz), 112.84("false t", *J* = 14.6 Hz), 108.72, 26.61, 24.64(t, *J* = 7.1 Hz), 24.21(t, *J* = 17.1 Hz), 14.02; ³¹P NMR (121 MHz, CDCl₃) δ 4.50 (*J*_{Pt-P} = 2337 Hz); IR (KBr) ν 2099.0 cm⁻¹ Pt-C≡C; EIMS calcd. [M+]⁺937.39; found [M+]⁺937; Anal. Calcd for C₄₂H₆₂F₆P₂Pt: C, 53.78%; H, 6.66%. Found: C, 53.92%; H, 5.56%.

CN: *trans*-Bis(tributylphosphine)-bis(4-cyano-phenylethynyl)platinum ¹H NMR (300 MHz, CDCl₃) δ 7.51(d, *J* = 8.4 Hz, 4H), 7.31(d, *J* = 8.4 Hz, 4H), 2.10(m, 12H), 1.60(m, 12H), 1.46(m, *J* = 7.2 Hz, 12H), 0.93(t, *J* = 7.2 Hz, 18H); ¹³C NMR (75 MHz, CDCl₃) δ 133.88, 132.03, 131.32, 119.80, 116.79("false t", *J* = 14.6 Hz), 109.34, 107.89, 26.59, 24.63(t, *J* = 6.8 Hz), 24.22(t, *J* = 17.1 Hz), 14.03; ³¹P NMR (121 MHz, CDCl₃) δ 4.63 (*J*_{Pt-P} = 2322 Hz); IR (KBr) ν 2098.0 cm⁻¹ Pt-C≡C; EIMS calcd. [M+]⁺851.98; found [M+]⁺852; Anal.

Calcd for $C_{42}H_{62}N_2P_2Pt$: C, 59.21%; H, 7.33%; N, 3.29%. Found: C, 59.17%; H, 7.16%; N, 3.13%.

NO_2 : *trans*-Bis(tributylphosphine)-bis(4-nitro-phenylethynyl)platinum 1H NMR (300 MHz, $CDCl_3$) δ 8.12(d, $J = 9.0$ Hz, 4H), 7.40(d, $J = 9.0$ Hz, 4H), 2.13(m, 12H), 1.62(m, 12H), 1.48(m, $J = 7.2$ Hz, 12H), 0.95(t, $J = 7.2$ Hz, 18H); ^{13}C NMR (75 MHz, $CDCl_3$) δ 144.84, 136.15, 131.18, 123.84, 119.35-("false t", $J = 14.6$ Hz), 109.87, 26.61, 24.62(t, $J = 6.6$ Hz), 24.29(t, $J = 17.1$ Hz), 14.01; ^{31}P NMR (121 MHz, $CDCl_3$) δ 4.78 ($J_{Pt-P} = 2314$ Hz); IR (KBr) ν 2096.0 cm^{-1} Pt-C \equiv C; EIMS calcd. $[M+]$ 891.96; found $[M+]$ 892; Anal. Calcd for $C_{40}H_{62}N_2O_4P_2Pt$: C, 53.86%; H, 7.01%; N, 3.14%. Found: C, 53.83%; H, 6.70%; N, 3.14%.

Extinction coefficients were measured from samples dissolved in methyl-tetrahydrofuran. A detailed study of linear, emission, and time-resolved spectroscopy will be published elsewhere. For two-photon absorption spectroscopy, all samples were prepared in tetrahydrofuran (THF) solution at chromophore concentration values in the range of 1–10 mM in standard 1 cm spectroscopic cuvettes. Degenerate instantaneous 2PA cross-section spectra were measured in the wavelength range of 550–900 nm utilizing a femtosecond optical parametric amplifier (OPERA, Coherent) pumped by a Ti:sapphire regenerative oscillator/amplifier (Libra, Coherent, Inc.). Because Pt-(R-X) $_2$ compounds studied here emit virtually no fluorescence, the 2PA measurements were performed using nonlinear transmission (NLT) method previously described.¹⁸

Briefly, the optical parametric amplifier (OPA) provided pulse energy up to 5–100 μJ per pulse (depending on wavelength) at 100 Hz pulse repetition rate. A thermoelectric optical power meter (Nova II, Ophir Inc.) was used to measure the average power. A diffraction grating spectrometer (USB4000, Ocean Optics) was used to measure the OPA spectrum, and a custom second harmonic generation autocorrelator was used to determine the pulse duration. The average spectral bandwidth and pulse duration were, respectively, $\Delta\lambda = 15$ –35 nm and 120–150 fs, depending on the wavelength. A linear polarizer along with a stack of color glass filters was used to block residual wavelengths in the OPA output. The OPA beam was slightly focused using long focal length lenses ($f = 500$ –1500 mm) to provide a spot size on the sample 300–1000 μm , again depending on wavelength. Two pick-off glass plates were placed at a distance of ~ 10 cm before and after the sample. The reflected light was directed to two integrating spheres equipped with silicon photodetectors (DET100A, Thorlabs). The OPA wavelength was tuned in 2 nm steps, and at each wavelength the incident pulse energy was varied in the range of $P_{in} = 0.2$ –20 μJ by using a personal computer (PC)-controlled variable reflective ND filter (Thorlabs). At each wavelength, the output signal of the two detectors was digitized using a DAQ card (PCI-6011, National Instruments, Inc.), and the data were analyzed using custom LabView routine, which evaluated the relative transmittance (defined as the ratio between the two integrated-over-the-pulse photodetector signals) as a function of the pulse energy. The intensity-dependent transmittance was fitted with a linear function, whereas to ensure validity of the linear fits, the maximum transmittance change was kept well below 5–10%. The two-photon absorption cross-section spectrum was obtained by comparing the slope of the fit function with respect to the slope obtained under the same excitation conditions using a known 2PA reference standard fluorescein in pH 11 H_2O . Estimated experimental uncertainty of the 2PA values is $\sim 20\%$.

Calculations were done using Gaussian 09W, Version 7.0.²¹ The chromophores were modeled as *trans*-Pt(PMe $_3$) $_2$ (C \equiv C-Phenyl-X) $_2$ in THF through use of polarizable continuum model (PCM). We performed DFT energy minimizations for the ground state using B3LYP/6-311g(2d,p) and TDDFT calculations using CAM-B3LYP/6-311g(2d,p). The basis set for the central Pt atom was SDD.

RESULTS AND DISCUSSION

Figure 1 shows ground-state absorption spectra of the compounds dissolved in methyl-tetrahydrofuran. Oscillator

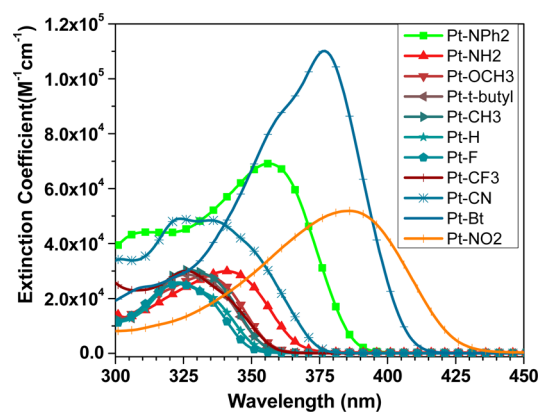


Figure 1. Ground-state absorption spectra of complexes dissolved in benzene.

strengths for the $S_0 \rightarrow S_1$ transition were calculated from a Gaussian fit to the low-lying ground-state spectra, and transition dipole moments were calculated from the relation

$$f_{01} = 4.70167 \times 10^{-7} \nu_{01} \mu_{01}^2 \quad (1)$$

where the transition frequency ν_{01} is in inverse centimeters, and the transition dipole moment μ_{01} is in debyes. The corresponding values are collected in Table 1.

Table 1. Summary of Ground-State Absorption Spectra

X	λ_{max}^a	ϵ_m^b	μ_{01}^c
NH $_2$	341	2.99	5.83
OCH $_3$	332	2.81	4.85
DPA	356	6.91	8.41
<i>t</i> -Bu	326	2.87	5.12
CH $_3$	327	3.04	5.31
H	323	2.58	4.37
F	323	2.53	4.57
BTH	377	11.0	10.9
CF $_3$	326	3.00	5.40
CN	335	4.84	7.71
NO $_2$	386	5.19	8.71

^aAbsorption maximum (nm). ^bExtinction coefficient ($(M^{-1} cm^{-1}) \times 10^{-4}$). ^cTransition dipole moment (D) obtained from Equation 1.

Figure 2 shows the 2PA cross-section spectra of the 11 compounds in THF solution. The 2PA cross section, σ_{2PA} , is expressed in Goeppert–Mayer units (1 GM = $1 \times 10^{-50} cm^4 photon^{-1} s$). Corresponding linear absorption spectra are also shown for comparison. With notable exception of NO_2 , the 2PA cross section of all compounds increases with decreasing excitation wavelength, λ_{2PA} , with maximum values reached at

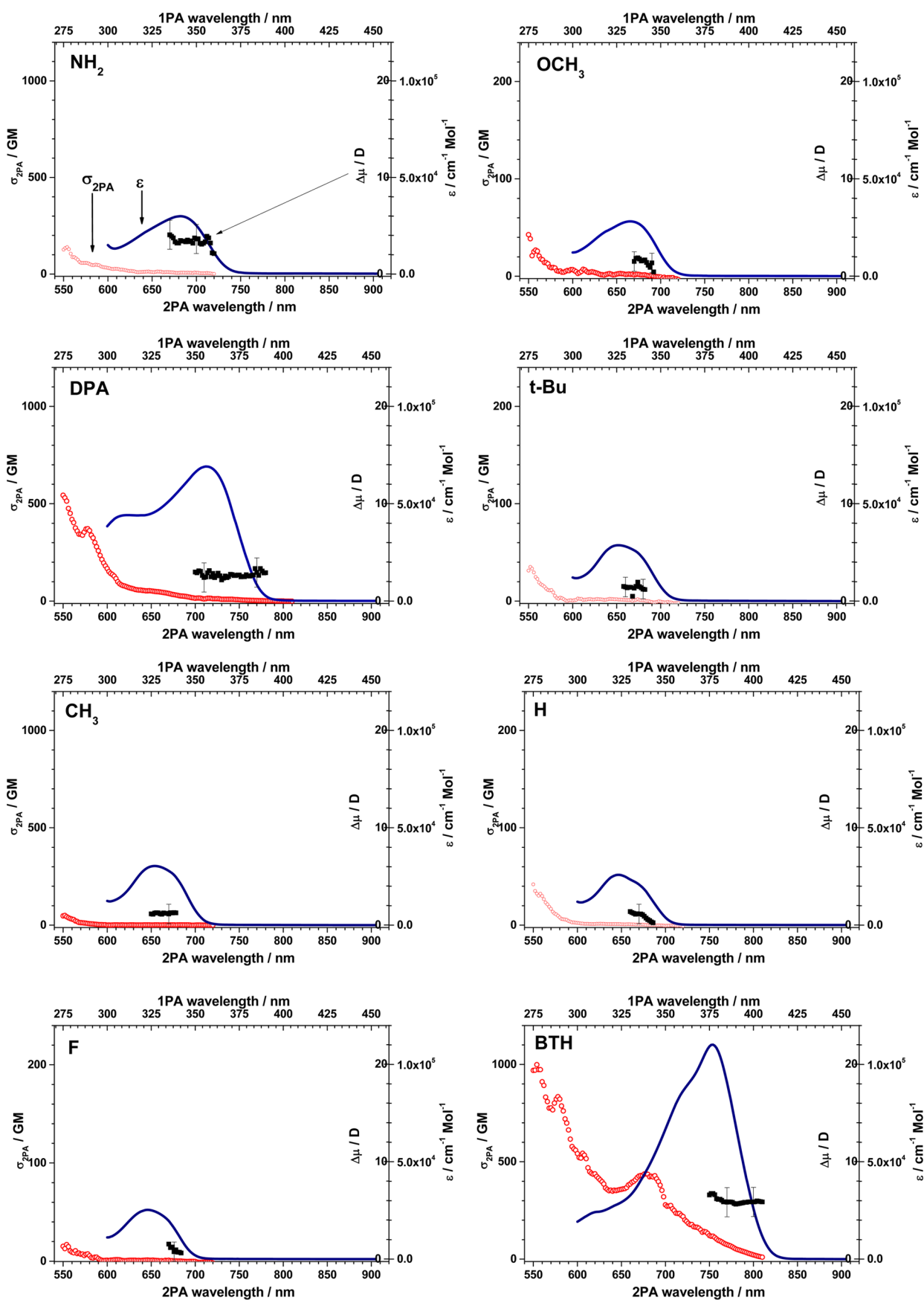


Figure 2. continued

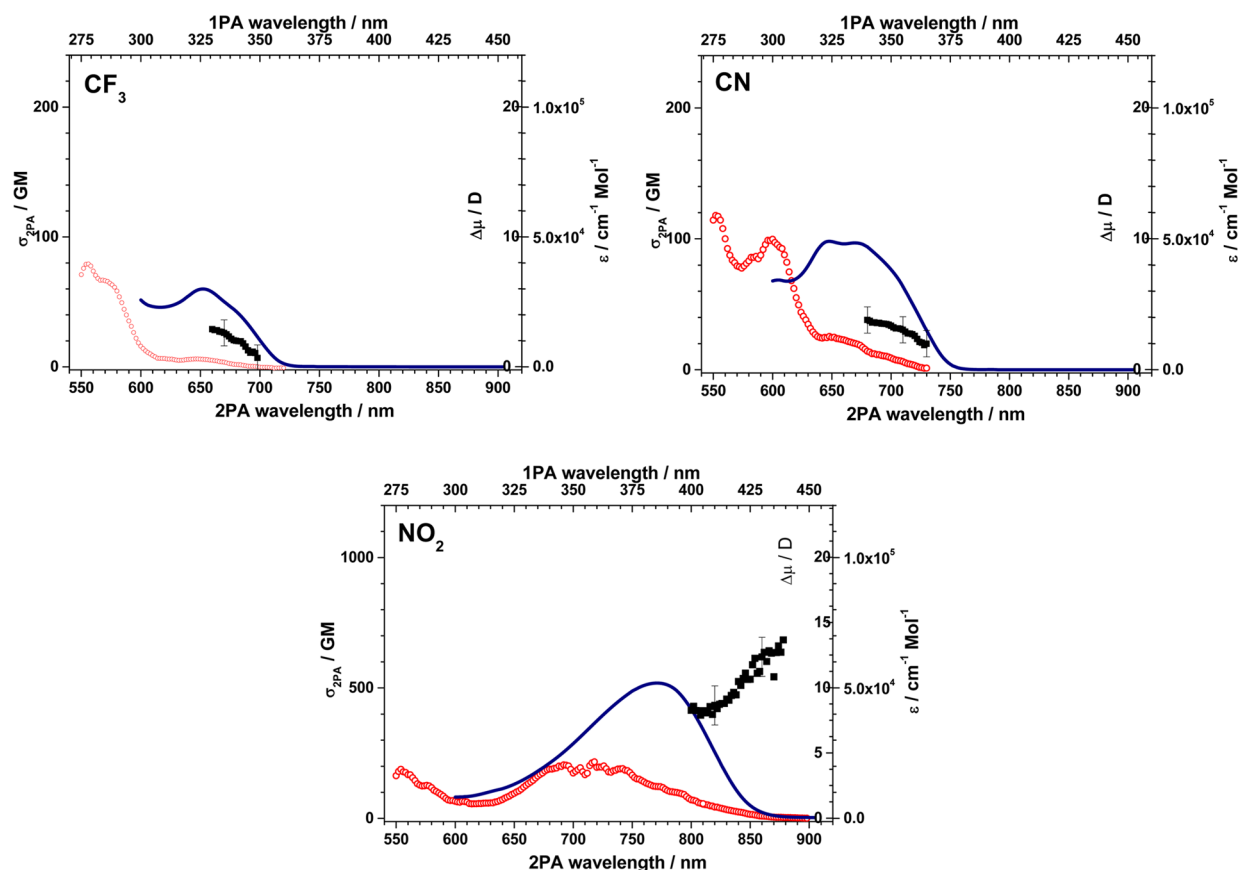


Figure 2. 2PA cross-section spectrum (red \circ , left vertical axis) of the 11 $\text{Pt}(\text{R-X})_2$ compounds in THF studied by the NLT method (left vertical axis). The ground-state extinction spectrum (blue line, right outside vertical axis) is shown for comparison. The lower and upper horizontal axes are calibrated in 2PA and 1PA wavelengths, respectively. (\blacksquare) $\Delta\mu$ values (inner right vertical axis) evaluated according to eq 2. As an example the spectra for compound NH_2 were labeled to help interpret the axis labels.

the shortest excitation wavelength, $\lambda_{2PA} < 650$ nm. This behavior may be attributed, in part, to conjugated organic chromophores often exhibiting the strongest two-photon transitions at energies, well above the $S_0 \rightarrow S_1$ band, and resonance enhancement effect via the lowest-energy dipole-allowed transition.¹⁶ From this perspective, the fact that the highest 2PA values in the whole series are observed in **BTH** ($\sigma_{2PA} \approx 1000$ GM) and in **DPA** ($\sigma_{2PA} \approx 600$ GM) at $\lambda_{2PA} = 550$ nm, correlates with higher-than-average transition dipole moments $\mu_{01} = 10.9$ and 8.4 D, respectively (Table 1). The resonance contribution to 2PA is likely further augmented because both chromophores exhibit a red-shifted $S_0 \rightarrow S_1$ band. In the remaining nine compounds, the maximum 2PA in the short wavelength region is substantially lower, $\sigma_{2PA} < 20\text{--}200$ GM, indicating that pronounced 2PA may occur at still higher energy that lies beyond current lower limit of 550 nm. We previously studied these effects in detail with the analogous $\text{Pt}(\text{FI-R-X})_2$ series, where we measured the 2PA spectra of the platinum complexes and the ligands.^{18,19} We also previously collected ultrafast transient absorption spectra of the $\text{Pt}(\text{FI-R-X})_2$ compounds.¹⁷ At higher transition energy corresponding to $S_0 \rightarrow S_n$ transition region, we find strong correlation between 2PA measured by the NLT method with excited state absorption (ESA) measured by pump-probe techniques. Because of weak ground-state absorption at 400 nm, we were unable to collect ESA spectra for the entire $\text{Pt}(\text{R-X})_2$ series. Ultrafast ESA spectra were measured for **H**, which was excited by femtosecond pulses at 340 nm.²² The intersystem crossing

time measured by fluorescence upconversion was estimated to be 70 fs. The ESA spectrum of **H** has broad absorption centered at 640 nm. In Figure 2, we observe increasing 2PA absorption from **H** at $\lambda < 600$ nm, which certainly includes ESA contribution.

Because the symmetry effects manifest most clearly in the lowest-energy transitions, especially in the 0–0 component of $S_0 \rightarrow S_1$ band, we will focus on the longest-wavelength portion of the 2PA spectrum. The σ_{2PA} of the 0–0 component of the $S_0 \rightarrow S_1$ transition, along with the corresponding wavelength, are shown in Table 2. These data show that σ_{2PA} corresponding to the 0–0 component of $S_0 \rightarrow S_1$ varies between 11 and 1 GM, whereas the latter value is most likely determined by upper accuracy limit of our experiment. If the angle θ between the two phenyl ring planes of $\text{Pt}(\text{R-X})_2$ is small, then the structure (Scheme 1) is nominally centrosymmetric, and one might expect that alternative parity selection rule must apply for one- and two-photon absorption spectra. Indeed, in case of **H**, **F**, and **CH₃**, 0–0 component of $S_0 \rightarrow S_1$ band that is strongly allowed in the linear absorption, is rather weak or even vanishing in the 2PA spectrum. However, in compounds decorated with potent electron-donating end groups and, in particular, those with strong electron-withdrawing substituents, the parity selection rule appears to be violated. This is especially evident in case of **NO₂**, where the one-photon and two-photon spectral profiles virtually coincide (Figure 2). Such behavior is common for strongly dipolar chromophores but not normally expected from systems possessing inversion symmetry. We evaluated the

Table 2. Summary of 2PA Cross Sections

X	Pt-(R-X) ₂ [S ₀ →S ₁ (0-0)]			Pt-(FL-R-X) ₂ [S ₀ →S ₁ (0-0)]		
	λ _{2PA} ^a	σ _{2PA} ^b	Δμ ^c	λ _{2PA} ^d	σ _{2PA} ^d	Δμ ^d
DPA	712	16	3	810	33	3.5
NH ₂	682	15	3.5	782	93	6.4
OCH ₃	668	10	1.5	774	57	5.5
<i>t</i> -butyl	672	1	1	772	73	6
CH ₃	670	1	1	774	61	5.3
H	672	1	1	774	92	7.5
F	668	1	1	772	53	5.5
CF ₃	684	2	1.5	792	120	7.5
CN	702	8	2	814	190	12
BT	752	120	6	826	270	12
NO ₂	774	120	11	862	700	25

^aTwo-photon absorption maximum (nm). ^bTwo-photon cross section (GM). ^cMeasured dipole moment change μ₁ - μ₀ (D) for S₁ state. ^dPublished two-photon absorption maximum, two-photon cross section, and dipole moment change for Pt-(FL-R-X)₂ system.¹⁸

change of permanent electric dipole in vertical S₀ → S₁ transition using the relation^{23,24}

$$\Delta\mu = 4550 \left(\frac{3}{n^2 + 2} \right) \sqrt{\frac{n\sigma_{2PA}(2\lambda)}{\lambda\epsilon_m(\lambda)}} \quad (2)$$

where *n* is the index of refraction of the solvent, λ is the wavelength of 0-0 component of S₀ → S₁ transition, and ε_m is the corresponding molar extinction (cm⁻¹ M⁻¹). Figure 2 shows Δμ (square symbols, right inner vertical axis) calculated according to eq 2 for 0-0 transition region in all 11 Pt-(R-X)₂ chromophores. In NH₂, OCH₃, DPA, *t*-Bu, CH₃, and BTH, Δμ is nearly constant, which is expected in case of a static electric dipole. But in some cases such as CF₃, CN, and NO₂, the value appears to change with the wavelength. There may be solvent complexes with the highly polar trifluoromethyl, nitrile, and nitro groups, which red-shift the 0-0 transition of a proportion of the solutes and change Δμ. To further understand these interactions, molecular dynamics simulations with explicit solvent-solute interactions followed by TDDFT calculations of properly sampled molecular conformations would need to be performed.²⁵ The average dipole moment values are summarized in Table 2. BTH and NO₂ exhibit the largest dipole moment change, 6 and 11 D, respectively. Also NH₂ and DPA show a pronounced dipole moment change Δμ ≈ 3 D. It is significant that the nonvanishing Δμ appears in vertical transitions from the electronic ground state. Since both one- and two-photon absorption are instantaneous quantum transition events with no time for any conformational changes, we conclude that inversion symmetry must be broken already in the ground state, that is, before the chromophore reaches the excited state. It is worth reminding that once in the excited-state manifold, changes of chromophore intrinsic symmetry are quite common, induced, for example, by vibrational relaxation, intersystem crossing, solvent rearrangement, etc. In the ground state, where the chromophore and its surrounding solvent are in equilibrium, spontaneous symmetry breaking is not so well-understood.

A qualitatively similar dependence of Δμ on the end-cap substituent structure was previously observed in the related series of Pt-(FL-R-X)₂.¹⁸ The corresponding data for of 0-0 component of S₀ → S₁ transition is reproduced in Table 2 for comparison. In both cases, NO₂ substituent appears to cause

the most pronounced symmetry-breaking effect, on the one hand because the corresponding values are the largest, and on the other hand because the shape of the 2PA spectrum switches to a distinctly dipolar character.

An explanation for the observed loss of inversion symmetry is nonplanar ground-state conformations. If the angle between the two phenyl ring planes is θ = 0°, then, by definition, Δμ = 0. However, if the rings are mutually rotated, then a finite electric dipole may occur. Table 3 summarizes the TDDFT calculations

Table 3. Summary of TDDFT Calculations^a

X	ΔE ^b	μ ₀₁ ^c	μ ₁ -μ ₀ ^d	ΔE ^e
NH ₂	3.99	8.59	2.98	0.03
OCH ₃	4.07	8.32	1.3	0.13
DPA	3.76	11.2	4.45	0.26
<i>t</i> -Bu	4.09	8.64	0.53	0.33
CH ₃	4.1	8.28	0.74	0.17
H	4.12	7.92	-0.07	0.22
F	4.14	7.73	0.5	0.17
BTH	3.53	14.9	3.69	0.34
CF ₃	4.06	8.87	2.69	0.34
CN	3.88	10.7	5.24	0.28
NO ₂	3.53	11.4	10.05	0.29

^aFor θ = 90°. ^bTransition energy in electronvolts for state 1. ^cTransition dipole in debyes for state 1. ^dDipole moment difference in debyes between S₁ state and ground state when θ = 90°. ^eGround-state energy difference ΔE = E_{gs}(θ = 90°) - E_{gs}(θ = 0°) in kilocalories per mole.

results regarding the transition energy, S₀ → S₁ transition dipole moment and Δμ in the case of θ = 90°. The S₁ state in all the calculations has predominantly highest occupied molecular orbital (HOMO) → lowest unoccupied molecular orbital (LUMO) character. The last column in Table 3 shows the calculated ground-state energy differences between θ = 0° and 90° conformations (in kcal mol⁻¹ units). Because the energy difference is much less than kT (0.6 kcal/mol) at room temperature, the calculations suggest that there is free rotation between the ligands, which means that statistically the chromophores are predominantly out-of-plane in solution, justifying our assumed rotation angle value, θ = 90°.

Figure 3 shows plots of calculated versus experimental S₁ state energies and transition dipole moments. The S₁ state energies and transition dipole moments obtained from the absorption spectra correlate very well with the calculations. The slopes are near unity, showing the calculations successfully describe the variation in energy and transition moment with substituent.

Figure 4 shows the effect of ligand length on Δμ. The left-hand portion of Figure 4 shows the experimental dipole moment change in the Pt-(R-X)₂ series (vertical axis) plotted as a function of Δμ values obtained previously in the Pt-(FL-R-X)₂ series (horizontal axis) with the same Pt core and the same 11 end-caps.¹⁸ The right-hand portion shows calculated Δμ values from Pt-(R-X)₂ vs Pt-(FL-R-X)₂. The linear fit to the data for both experimental and calculated dipole moment changes (red line) has the slope ~0.5 because the absolute dipole moment values are ~2 times larger in the Pt-(FL-R-X)₂ compounds, which may be related to the conjugation, and intramolecular charge transfer extends over a larger distance compared to the shorter Pt-(R-X)₂ series. Aside from the difference in absolute values, there is good correlation between

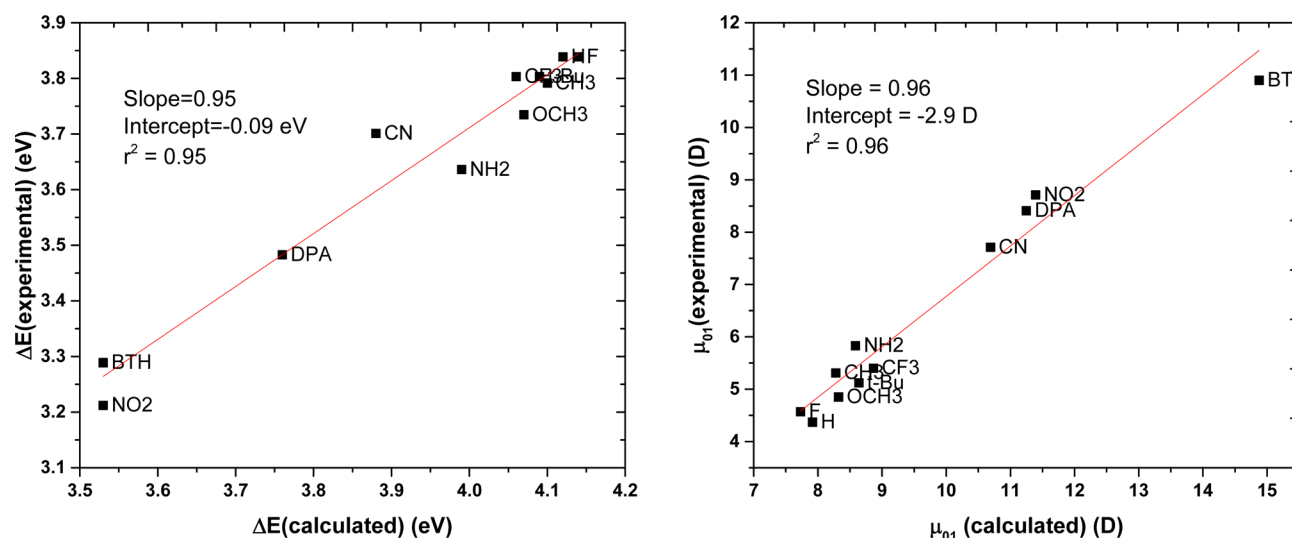


Figure 3. (left) Plot of calculated vs experimental S_1 state transition energies. (right) Plot of calculated vs experimental transition dipole moments.

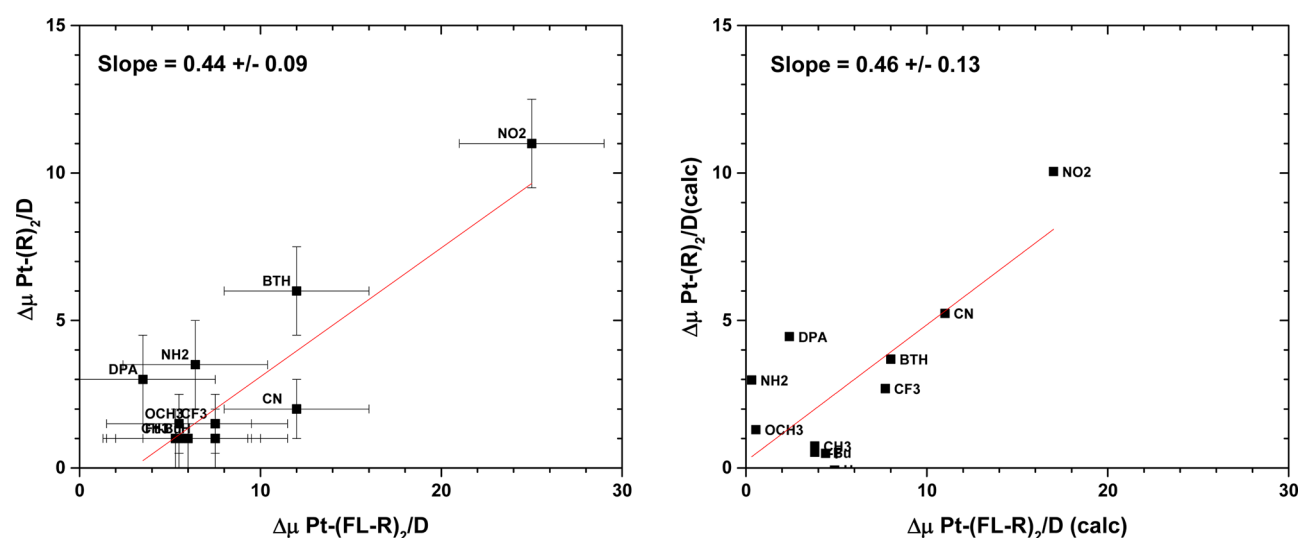


Figure 4. (left) Experimental $\Delta\mu$ in the $\text{Pt}-(\text{R}-\text{X})_2$ series (vertical axis) plotted as a function of $\Delta\mu$ values obtained previously in the $\text{Pt}-(\text{FL}-\text{R}-\text{X})_2$ series¹⁸ with the same Pt core and the same 11 end-caps, but additional fluorenyl linker inserted between the core and the end-caps; (right) calculated $\Delta\mu$ values from $\text{Pt}-(\text{R}-\text{X})_2$ vs $\text{Pt}-(\text{FL}-\text{R}-\text{X})_2$.¹⁸

dipole moments for the same end cap. From these observations we can conclude that in both series $\Delta\mu$ is determined by the nonplanar molecular conformation, the electronic properties of the end caps, and the length of the spacer group. There is recent literature describing systems in which, upon excitation, a nominally quadrupolar chromophore behaves like an excited-state dipole.^{26–29} Provided the ground-state conformation is rigid, the time-resolved spectroscopic data can be interpreted as relaxation to a dipolar excited state. In the current system, the centrosymmetric chromophores have a floppy ground-state conformation, which gives then dipolar excited-state behavior.

CONCLUSIONS

In this work we synthesized a series of chromophores $\text{trans-Pt}(\text{PBu}_3)_2(\text{C}\equiv\text{C-Phenyl-X})_2$, where $\text{X} = \text{NH}_2, \text{OCH}_3, \text{DPA}, t\text{-Bu}, \text{CH}_3, \text{H}, \text{F}, \text{BTH}, \text{CF}_3, \text{CN},$ and NO_2 . We collected ground-state absorption and two-photon spectra. We also performed DFT and TDDFT calculations on the ground and excited-state properties of these compounds. The calculations

show the energy difference between the $\theta = 90^\circ$ versus $\theta = 0^\circ$ is less than kT , suggesting the compounds in solution have a statistical mix of out-of-plane conformations. When $\theta = 90^\circ$, there is good agreement between calculated and experimental S_1 state energies, transition dipole moments, and excited-state dipole moments. The spectroscopy and calculation results suggest these chromophores have very flexible structure, and out-of-plane conformation predominates in solution. The ground-state and 2PA absorption spectra result from symmetry-broken ground-state out-of-plane conformations.

AUTHOR INFORMATION

Corresponding Authors

*E-mail: Thomas.Cooper.13@us.af.mil. (T.M.C.)

*E-mail: rebane@physics.montana.edu. (A.R.)

ORCID

Thomas M. Cooper: 0000-0002-4635-8281

Notes

The authors declare no competing financial interest.

ACKNOWLEDGMENTS

We are thankful for the support of this work by AFRL/RX Contract Nos. F33615-03-D-5408 for D.M.K. and A.R.B., F33615-03-D-5421 for J.E.S., and FA9550-09-1-0219 for A.R.B.; A.R. and A. M. are supported by AFOSR Grant No. FA9550-16-1-0189. We thank A. Shelton, Univ. of Florida, for collection of ground-state absorption spectra and G. Wicks for help in collecting two-photon absorption spectra.

REFERENCES

- (1) Rogers, J. E.; Cooper, T. M.; Fleitz, P. A.; Glass, D. J.; McLean, D. G. Photophysical Characterization of a Series of Platinum(II)-Containing Phenyl-Ethynyl Oligomers. *J. Phys. Chem. A* **2002**, *106*, 10108–10115.
- (2) Yam, V. W.-W.; Au, V. K.-M.; Leung, S. Y.-L. Light-Emitting Self-Assembled Materials Based on d8 and d10 Transition Metal Complexes. *Chem. Rev.* **2015**, *115*, 7589–7728.
- (3) Rogers, J. E.; Hall, B. C.; Hufnagle, D. C.; Slagle, J. E.; Ault, A. P.; McLean, D. G.; Fleitz, P. A.; Cooper, T. M. Effect of Platinum on the Photophysical Properties of a Series of Phenyl-ethynyl Oligomers. *J. Chem. Phys.* **2005**, *122*, 214708–214715.
- (4) Cooper, T. M.; Krein, D. M.; Burke, A. R.; McLean, D. G.; Rogers, J. E.; Slagle, J. E.; Fleitz, P. A. Spectroscopic Characterization of a Series of Platinum Acetylide Complexes Having a Localized Triplet Exciton. *J. Phys. Chem. A* **2006**, *110*, 4369–4375.
- (5) Cooper, T. M.; Krein, D. M.; Burke, A. R.; McLean, D. G.; Rogers, J. E.; Slagle, J. E. Asymmetry in Platinum Acetylide Complexes: Confinement of the Triplet Exciton to the Lowest Energy Ligand. *J. Phys. Chem. A* **2006**, *110*, 13370–13378.
- (6) Silverman, E. E.; Cardolaccia, T.; Zhao, X.; Kim, K.-Y.; Haskins-Gluscak, K.; Schanze, K. S. The Triplet State in Pt-Acetylide Oligomers, Polymers and Copolymers. *Coord. Chem. Rev.* **2005**, *249*, 1491–1500.
- (7) Kohler, A.; Wilson, J. S. Phosphorescence and Spin-dependent Exciton Formation in Conjugated Polymers. *Org. Electron.* **2003**, *4*, 179–189.
- (8) Wong, W.-Y.; Ho, C.-L. Di-, Oligo- and Polymetallaynes: Syntheses, Photophysics, Structures and Applications. *Coord. Chem. Rev.* **2006**, *250*, 2627–2690.
- (9) Cooper, T. M.; Ziolo, R. F.; Burke, A. R.; Glushchenko, A. V. Glassy Cholesteric Liquid Crystalline Metal Acetylides. *U.S. Pat. Appl. Publ.* 2014, US 20140242344 A1 20140828.
- (10) Rogers, J. E.; Slagle, J. E.; Krein, D. M.; Burke, A. R.; Hall, B. C.; Fratini, A.; McLean, D. G.; Fleitz, P. A.; Cooper, T. M.; Drobizhev, M.; Makarov, N. S.; Rebane, A.; Kim, K.-Y.; Farley, R.; Schanze, K. S. Platinum Acetylide Two-Photon Chromophores. *Inorg. Chem.* **2007**, *46*, 6483–6494.
- (11) Dubinina, G. G.; Price, R. S.; Abboud, K. A.; Wicks, G.; Wnuk, P.; Stepanenko, Y.; Drobizhev, M.; Rebane, A.; Schanze, K. S. Phenylene Vinylene Platinum(II) Acetylides with Prodigious Two-Photon Absorption. *J. Am. Chem. Soc.* **2012**, *134*, 19346–19349.
- (12) Vivas, M. G.; De Boni, L.; Cooper, T. M.; Mendonca, C. R. Understanding the Two-Photon Absorption Spectrum of PE2 Platinum Acetylide Complex. *J. Phys. Chem. A* **2014**, *118*, 5608–5613.
- (13) Vivas, M. G.; De Boni, L.; Cooper, T. M.; Mendonca, C. R. Interpreting Strong Two-Photon Absorption of PE3 Platinum Acetylide Complex: Double Resonance and Excited State Absorption. *ACS Photonics* **2014**, *1*, 106–113.
- (14) Vivas, M. G.; Piovesan, E.; Silva, D. L.; Cooper, T. M.; De Boni, L.; Mendonca, C. R. Broadband Three-Photon Absorption Spectra of Platinum Acetylide Complexes. *Opt. Mater. Express* **2011**, *1*, 700–710.
- (15) Slagle, J. E.; Cooper, T. M.; Krein, D. M.; Rogers, J. E.; McLean, D. G.; Urbas, A. M. Triplet Excimer Formation in a Platinum Acetylide. *Chem. Phys. Lett.* **2007**, *447*, 65–68.
- (16) Slagle, J. E.; Haus, J. W.; Guha, S.; McLean, D. G.; Krein, D. M.; Cooper, T. M. Degenerate Frequency Two-Beam Coupling in Organic Media via Phase Modulation with Nanosecond Pulses. *J. Opt. Soc. Am. B* **2016**, *33*, 180–188.
- (17) Haley, J. E.; Krein, D. M.; Monahan, J. L.; Burke, A. R.; McLean, D. G.; Slagle, J. E.; Fratini, A.; Cooper, T. M. Photophysical Properties of a Series of Electron-Donating and Withdrawing Platinum Acetylide Two-Photon Chromophores. *J. Phys. Chem. A* **2011**, *115*, 265–273.
- (18) Rebane, A.; Drobizhev, M.; Makarov, N. S.; Wicks, G.; Wnuk, P.; Stepanenko, Y.; Haley, J. E.; Krein, D. M.; Fore, J. L.; Burke, A. R.; Slagle, J. E.; McLean, D. G.; Cooper, T. M. Symmetry Breaking in Platinum Acetylide Chromophores Studied by Femtosecond Two-Photon Absorption Spectroscopy. *J. Phys. Chem. A* **2014**, *118*, 3749–3759.
- (19) Rebane, A.; Drobizhev, M.; Makarov, N. S.; Beuerman, E.; Haley, J. E.; Krein, D. M.; Burke, A. R.; Flikkema, J. L.; Cooper, T. M. Relation Between Two-Photon Absorption and Dipolar Properties in a Series of Fluorenyl-Based Chromophores with Electron-Donating or Electron-Withdrawing Substituents. *J. Phys. Chem. A* **2011**, *115*, 4255–4262.
- (20) Dereka, B.; Rosspeintner, A.; Vauthey, E.; Krzeszewski, M.; Gryko, D. T. Symmetry-Breaking Charge Transfer and Hydrogen Bonding: Toward Asymmetrical Photochemistry. *Angew. Chem., Int. Ed.* **2016**, *55*, 15624–15628.
- (21) Frisch, M. J.; Trucks, G. W.; Schlegel, H. B.; Scuseria, G. E.; Robb, M. A.; Cheeseman, J. R.; Montgomery, J. A.; Vreven, T.; Kudin, K. N.; Burant, J. C. et al. *Gaussian 09*, Revision B.05; Gaussian, Inc.: Pittsburgh, PA, 2009.
- (22) Ramakrishna, G.; Goodson, T., III; Rogers-Haley, J. E.; Cooper, T. M.; McLean, D. G.; Urbas, A. Ultrafast Intersystem Crossing: Excited State Dynamics of Platinum Acetylide Complexes. *J. Phys. Chem. C* **2009**, *113*, 1060–1066.
- (23) Drobizhev, M.; Karotki, A.; Kruk, M.; Rebane, A. Resonance Enhancement of Two-Photon Absorption in Porphyrins. *Chem. Phys. Lett.* **2002**, *355*, 175–182.
- (24) Rebane, A.; Wicks, G.; Drobizhev, M.; Cooper, T.; Trummal, A.; Uudsemaa, M. Two-Photon Voltmeter for Measuring a Molecular Electric Field. *Angew. Chem., Int. Ed.* **2015**, *54*, 7582–7586.
- (25) Sjöqvist, J.; Linares, M.; Norman, P. Platinum(II) and Phosphorus MM3 Force Field Parametrization for Chromophore Absorption Spectra at Room Temperature. *J. Phys. Chem. A* **2010**, *114*, 4981–4987.
- (26) Ivanov, A. I.; Dereka, B.; Vauthey, E. A. Simple Model of Solvent-Induced Symmetry-Breaking Charge Transfer in Excited Quadrupolar Molecules. *J. Chem. Phys.* **2017**, *146*, 164306.
- (27) Ricci, F.; Carlotti, B.; Keller, B.; Bonaccorso, C.; Fortuna, C. G.; Goodson, T.; Elisei, F.; Spalletti, A. Enhancement of Two-Photon Absorption Parallels Intramolecular Charge-Transfer Efficiency in Quadrupolar versus Dipolar Cationic Chromophores. *J. Phys. Chem. C* **2017**, *121*, 3987–4001.
- (28) Dereka, B.; Rosspeintner, A.; Li, Z.; Liska, R.; Vauthey, E. Direct Visualization of Excited-State Symmetry Breaking Using Ultrafast Time-Resolved Infrared Spectroscopy. *J. Am. Chem. Soc.* **2016**, *138*, 4643–4649.
- (29) Dereka, B.; Koch, M.; Vauthey, E. Looking at Photoinduced Charge Transfer Processes in the IR: Answers to Several Long-Standing Questions. *Acc. Chem. Res.* **2017**, *50*, 426–434.